N78-24061

CHARACTERISTICS OF USB NOISE*

J. S. Gibson and N. Searle
Lockheed-Georgia Company

SUMMARY

An extensive series of noise measurements, for a variety of geometric and operational parameters, have been made on models of upper surface blowing (USB) powered-lift systems. The data obtained have been analyzed and the effects and trends of parametric variation have been defined. From these results, insight can be gained into the behavior and nature of USB noise and the design of USB systems with low noise characteristics.

INTRODUCTION

This paper is concerned with the USB parametric acoustic evaluation program that is a companion effort to the flow field work described in the preceding paper, and the analytical acoustics work which is given in the next paper. In this discourse, primary emphasis is placed on observed far field acoustic effects and trends resulting from geometric and operational parameter variations. Most of the results to be covered relate to static, cold flow, blended nacelle, upper surface blowing configurations. The majority of the results are for attached flow cases; however, also briefly covered are some separated flow cases, as well as some vectored thrust cases, flow temperature effects, and forward speed effects.

EXPERIMENTAL FACILITIES

The majority of the acoustic data were obtained in an anechoic room, illustrated in figure 1. The small scale USB model which has a 51 cm (20 in.) wing span is shown inverted and mounted to the end of a foam-covered muffler and air pipe system. This is the same model that is described in the preceding paper. Several microphone arches, each on a 2.44 meter (8 ft.) radius, can also be seen, as well as the room itself. Noise measurements were made at many locations, but the typical experimental trends discussed in this paper were taken from the microphone directly opposite the bottom of the wing, unless otherwise stated. This location corresponds to an observer located directly under an aircraft.

* Work performed under NASA Contract NAS1-13870 with NASA-Langley Research Center.

15

The outdoor facility, which accepts models larger by approximately a factor of two and a half, is shown in figure 2. Parametric data primarily for scaling purpose were obtained at this facility. The model, also described in the preceding paper, is mounted in the center of the test pad, being fed by a muffled piped air supply. The moveable, motorized 6.1 meter (20 ft.) radius microphone arch, model air supply, and all data acquisition systems are remotely controlled from a control room located in the building in the background.

The final facility used in this program is the anechoic wind tunnel shown in figure 3. This is a 0.76 x 1.09 meter (30 x 43 inches), continuous free-jet type facility. Tunnel air flow is from left to right into the foam lined collector. The model, which is the same size and uses the same flaps as the static anechoic room and flow study model, can be seen mounted to a fairing just inside the tunnel flow field. The nozzle is fed from a muffled pipe which goes along the upstream tunnel centerline.

ATTACHED FLOW PARAMETRIC AND OTHER NOISE CHARACTERISTICS

The parametric results presented in this section are for attached flow conditions, except for those few cases discussed under the heading of "separated flow effects." As mentioned previously, the trends shown in the figures are derived from typical data at a location which simulates an observers position directly under an aircraft. Trends at this location, in most cases, are similar to trends at other points below the wing as well.

Nozzle Exit Velocity

Nozzle exit velocity has a major effect on USB noise. Both noise level and peak frequency increase as jet velocity increases. As indicated in figure 4, the peak frequency effect has been collapsed into non-dimensional form by converting the frequency scale to Strouhal number, where f is the frequency in Hertz, V_j is jet exit velocity, and L_f is nozzle to flap trailing edge flow length. The spectral data shown are for a series of jet velocities with all other parameters constant. In Strouhal form, the spectrum shapes are similar. The level of noise at any frequency is typically proportional to $V_j^{5.5}$ directly under the model; proportional to $V_j^{5.0}$ in the forward quadrant; and varies to $V_j^{7.5}$ in the extreme aft quadrant.

Nozzle Shape

Figure 5 shows the effect of nozzle shape. This figure is in conventional one-third octave band form. The very low and high frequency range of the spectra are essentially independent of nozzle shape. However, the relatively narrow peak frequency range is significantly affected. The trend is higher levels for lower aspect ratio nozzles. The variation is over about a 5 dB range between a round nozzle and an aspect ratio (AR) 8 rectangular nozzle. These effects are slightly greater in the aft quadrant. The conclusion here is that the more spread out on the flaps a given amount of jet flow is, the less noise is generated in the peak frequency region. The reason why only the peak frequency range is affected is currently unknown. It may be associated with the flow field edge roll-up vortices, which are larger and stronger for lower nozzle aspect ratios.

It should be pointed out that these peak spectrum effects would occur at rather low frequencies on a full scale aircraft and may have more of an aircraft structural vibration and interior sound proofing impact than a community noise impact.

Nozzle Impingement Angle

The result of impinging the nozzle at successively higher angles with respect to the wing is somewhat similar to increasing nozzle aspect ratio. As the angle is increased, the flow is spread out more over the wing and flaps. The noise spectrum, as can be seen in figure 6, is affected significantly only in the mid-frequency range, where lower noise levels correspond to higher impingement angles. The peak noise level varies over about a 5 dB range as in the case of nozzle shape. These data, as well as the nozzle shape data, have been corrected to a constant flow rate.

Flow Path Length

The subject of flow path length is involved with two geometric parameters - nozzle horizontal location on the wing and flap trailing edge length. Either parameter changes the total flow path length between the nozzle exit plane and the flap trailing edge. As flow length increases, higher frequency noise decreases regardless of which of the two parameters' length was varied. As can be seen in figure 7, the data from several examples of nozzle location and trailing edge length variation collapse rather well when the frequency scale is converted to Strouhal number form with total flow length, L_f, as the characteristic dimension. The apparent exception is the noticeable peak in the 50% chord data. However, this peak is due to an aeroacoustic resonance phenomenon (a tone or whistle sound) that appeared sporadically in the experimental program. Resonances of this type were related to flow disturbances near the beginning of the flap radius section, feeding back energy to the nozzle exit plane instability area. They are apparently a function of wing-flap joint smoothness rather than any of the basic parametric variables. When the surface was smoothed, the tone disappeared and the anomalus peak then collapsed with the other data in figure 7.

Flap Radius of Curvature

While flow path length is an important parameter, the shape of the path is apparently not important at all to noise for attached flow. Over a wide range of flap knee radius of curvature, no systematic trend could be found and the variations observed were inconsequential. This corresponds to the results of the companion flow field study where radius of curvature had a small effect, in fact the smallest effect of any of the experimental variables.

Even in cases where flow separation "bubbles" were noted on the flap, no significant noise trend was seen as long as the flow reattached prior to leaving the trailing edge.

Flap Angle

Flap angle is one of the more obvious variables in a USB system, but it has a rather small effect on noise under the wing. There is mainly a low frequency shift, or increase, as indicated in figure 8. The sound field, or directivity pattern, moves with the flap as the flap is rotated downward. However, this directivity effect is relatively insensitive over the 60° range investigated.

Jet Temperature

A limited investigation of jet temperature was performed. As indicated in figure 9, when the temperature is increased from 24°C (75°F) over a range of jet velocities, the overall noise levels drop, stay the same, or increase. To convert these results to constant thrust conditions, the 93°C (200°F) data should be shifted up about 1 dB. Actually the velocity exponent is reduced when the temperature is increased, thereby changing the slope of the noise versus velocity curve. In this case, the low temperature curve was proportional to $V_j^{5.6}$ and the high temperature curve was proportional to $V_j^{4.8}$. These relationships are somewhat different at other microphone locations as were the basic jet velocity trends with location as mentioned previously.

Vectored Thrust

In addition to the blended type nacelle, the use of over-the-wing pylon mounted nacelles with vectored down jet flows for low speed performance shows promise as a viable powered lift configuration. Up to this point, only the blended or fully integrated nacelle and wing installations have been discussed. Figure 10 shows how a typical vectored installation compares with the blended type. In general, as the exhaust nozzle is brought up from the wing surface, and vectored downward, noise throughout most of the spectrum increases and the spectrum shape broadens. The largest changes occur in the high frequency range which could affect community noise since subjective noise ratings are more sensitive to high frequency noise. The example shown is for a nozzle vector angle of 40° where the nozzle height, or gap between the nozzle and wing surface, was 30% of the nozzle diameter. For lower vector angles and lower nozzle heights the noise increases are smaller. This is really a rather complex situation needing more study since our investigation was limited in the number of configurations tested.

Scaling Trends

Figure 11 indicates that, over the range of a factor of two and a half in model size that was utilized in this program, spectral scaling is rather good based on linear size and velocity factors for the frequency scale, and on 10 Log nozzle area ratio for the noise level scale (as was done in this figure). Therefore, basic USB noise scaling apparently behaves in the same manner as normal subsonic jet noise, a conclusion that has also been observed by other investigators.

We also had one case where the wing, flap, and other parameters were kept constant, except that the nozzle area was reduced by a factor of two (round nozzles in both instances). A negligible spectrum effect was noted and the overall noise level scaled as in the small versus large complete model example.

Separated Flow Effects

All of the results to this point have had flow attachment at the trailing edge and reasonably good flow turning. To determine what effect poor attachment and turning would have, a special series of test runs were made and the trends illustrated in figure 12. The upper curve is a typical attached flow case, where the nozzle was flush mounted on the wing with a nozzle impingement angle of 10°. The middle curve is for a case where everything is the same, except the nozzle impingement angle was reduced to 0°, causing the flow to separate just upstream of the trailing edge. These are low-and mid-frequency noise reductions, but the high-frequency range is about the same. This result helps to substantiate the idea that much of the low-frequency noise of a USB system is related to flow - trailing edge interaction. The lower curve is for a case where the nozzle is above the wing and the flow is not vectored down. This results in the jet flow being completely unattached and not turned down at all. The corresponding noise levels across the spectrum are reduced, due to no flow - structure interaction and no downward turning of the jet noise directivity pattern.

Effect of Forward Speed

A short series of tests were run in the anechoic wind tunnel to obtain some data on the effect of forward speed on USB noise. Typical results are as indicated in figure 13. At low frequency, up to the peak, there is a noise decrease with forward speed of several dB, about 4 dB in this particular case. However, throughout the mid- and high-frequency range, there is only about a 0.5 dB reduction. These trends are largely independent of observer location and are also similar for a 60° flap case, as well as for an over-the-wing vectored nozzle case that was run. The reasons for these results are still under investigation.

CONCLUDING REMARKS

It has been shown that the primary variables controlling far field noise for attached flow USB systems are jet velocity, flow path length, and nozzle vertical location. Other parameters, including flap angle, nozzle shape, nozzle impingement angle, and jet temperature also have noticeable and systematic effects, but are generally considered of secondary importance for far field or community noise. Those several parameters causing low-frequency noise increases, however, will undoubtedly increase the aircraft problems of structural vibration, sonic-fatigue, and passenger compartment noise.

Noise results have been presented independently of quantitative aeropropulsion performance effects. A study of the tradeoffs between low noise design features and good aircraft performance is a phase of the program that is not complete at the time of this writing. Therefore, the use of the noise trends alone in a USB aircraft design study should be done with care so that low noise features will not be offset by aircraft performance penalties.

Finally, it should be noted that not all the acoustic effects we have observed can be explained with any degree of satisfaction. There is still much to be learned about the basic nature of USB noise and realistic USB nozzle-wing-flap installations for optimum low noise airplane design.

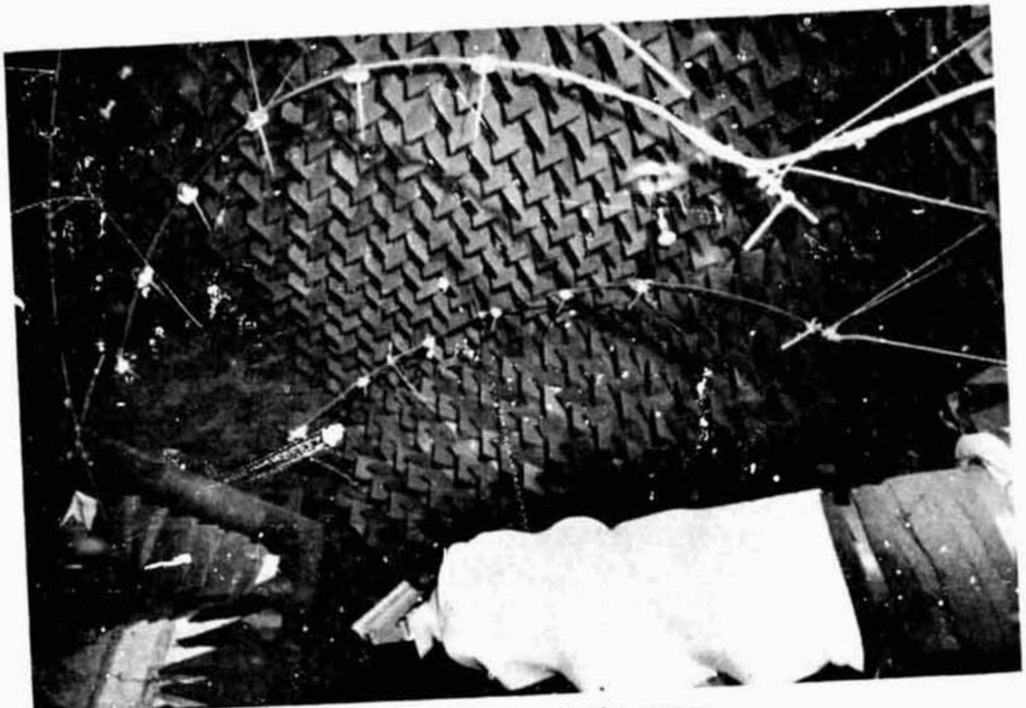

Figure 1.- Anechoic room.

Figure 2.- Outdoor facility.

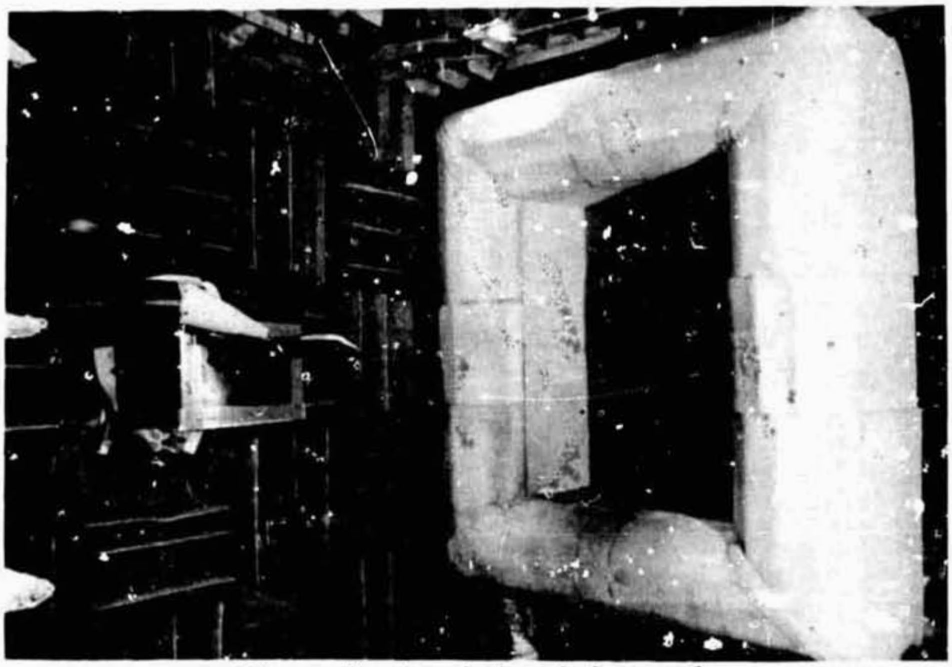

Figure 3.- Anechoic wind tunnel.

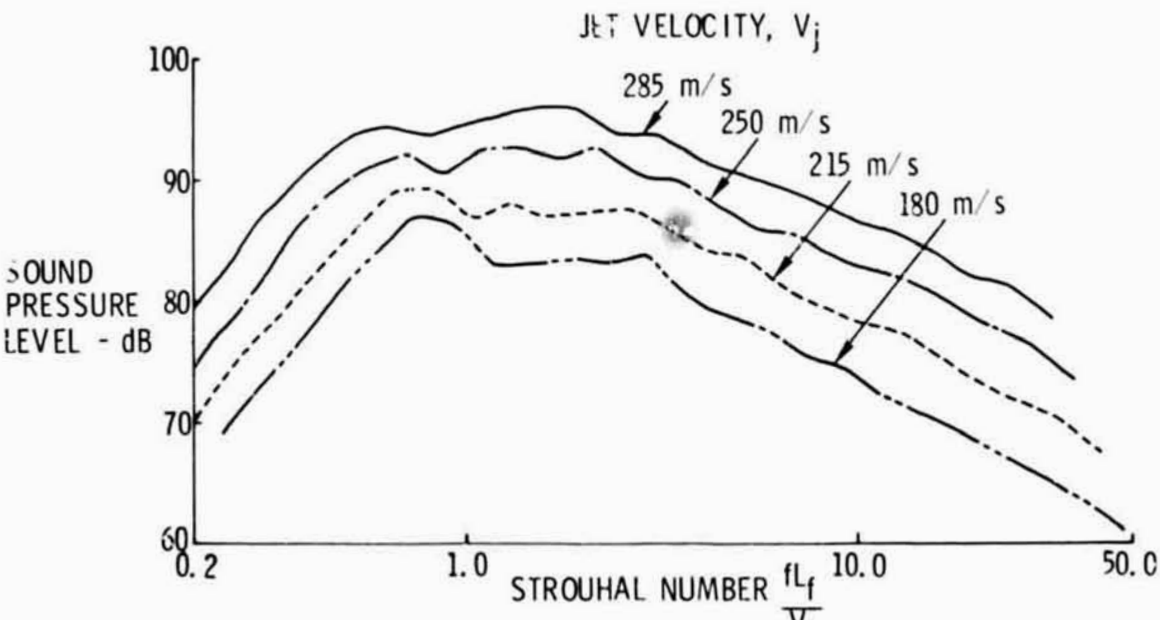

Figure 4.- Effect of jet velocity. AR4 nozzle; nozzle impingement angle 20°; nozzle location 20% chord; flap angle 30°.

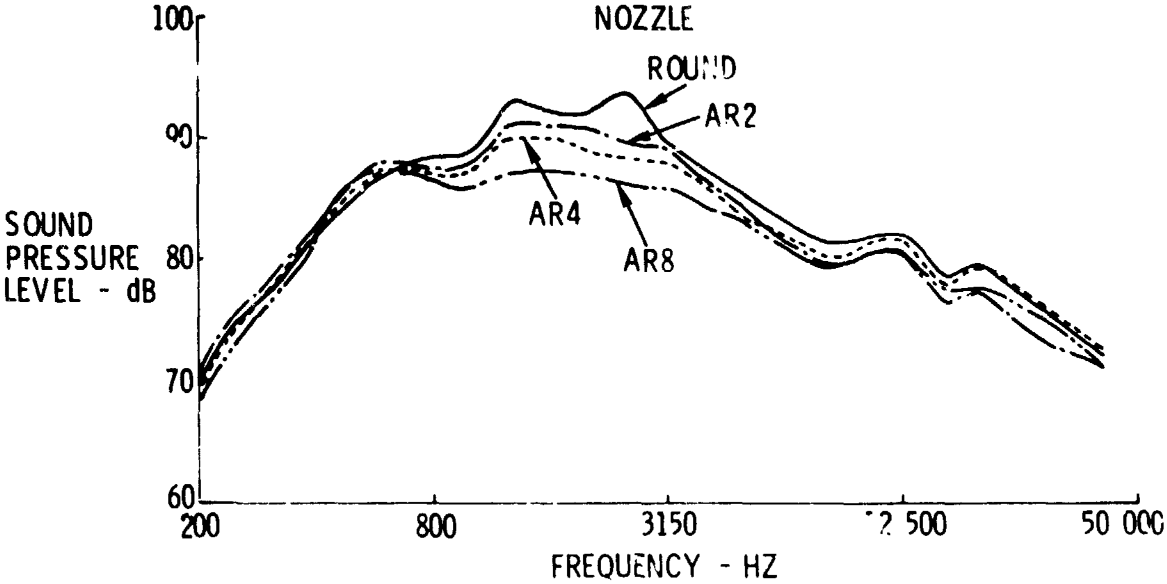

Figure 5.- Effect of nozzle shape. Jet velocity 215 m/s; nozzle location 20% chord; nozzle impingement angle 20°; flap angle 30°.

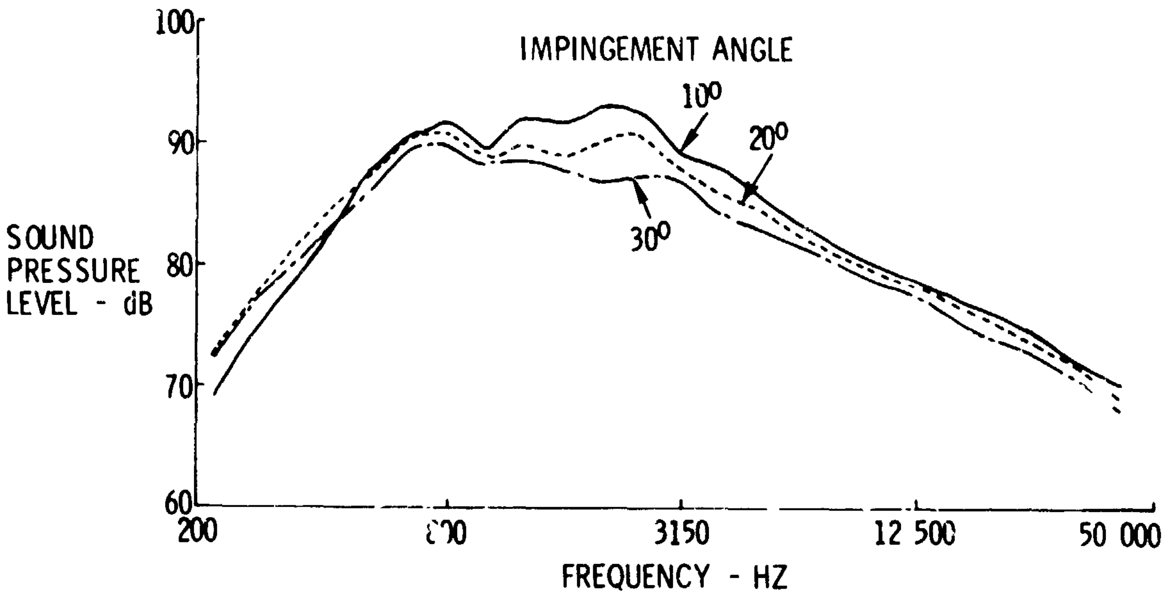

Figure 6.- Effect of nozzle impingement angle. AR4 nozzle; jet velocity 215 m/s; nozzle location 20% chord; flap angle 30°.

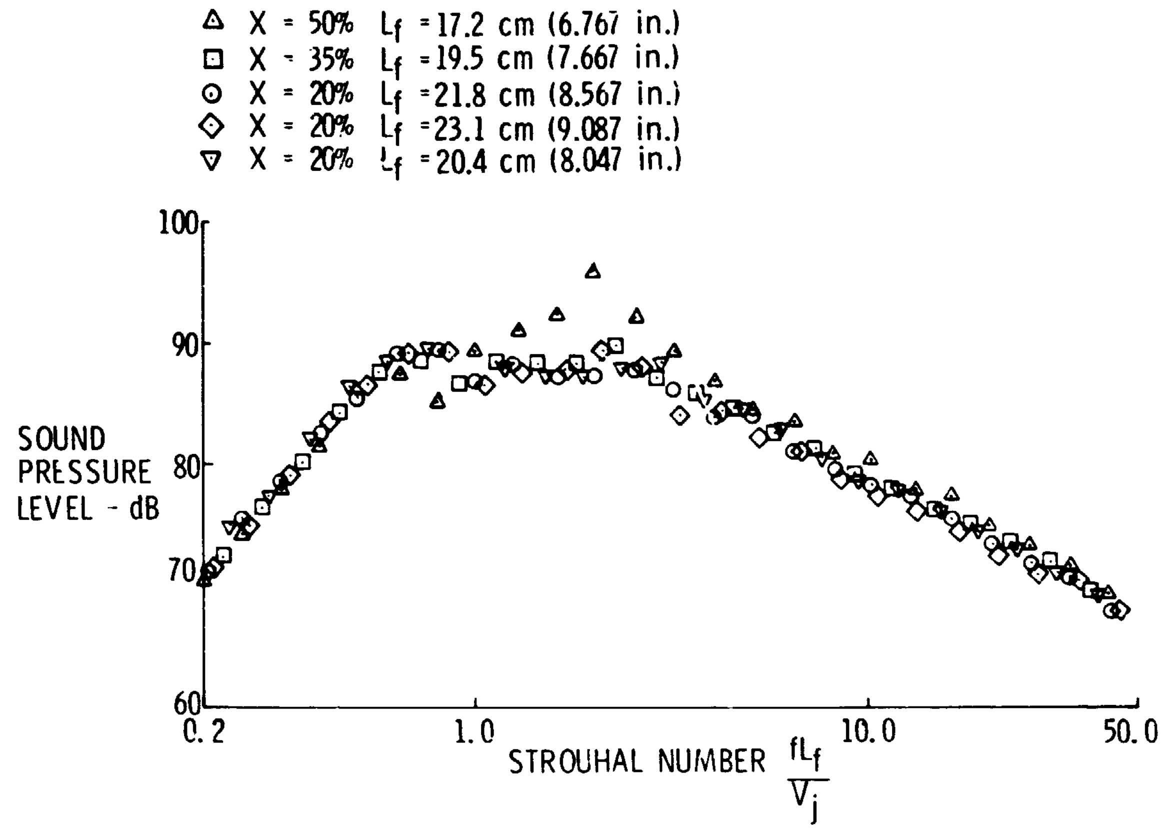

Figure 7.- Effect of flow path length. Jet velocity, V_j, 215 m/s; AR4 nozzle; nozzle impingement angle 20°; flap angle 30°; nozzle location, X, and flow path length, L_f, as indicated.

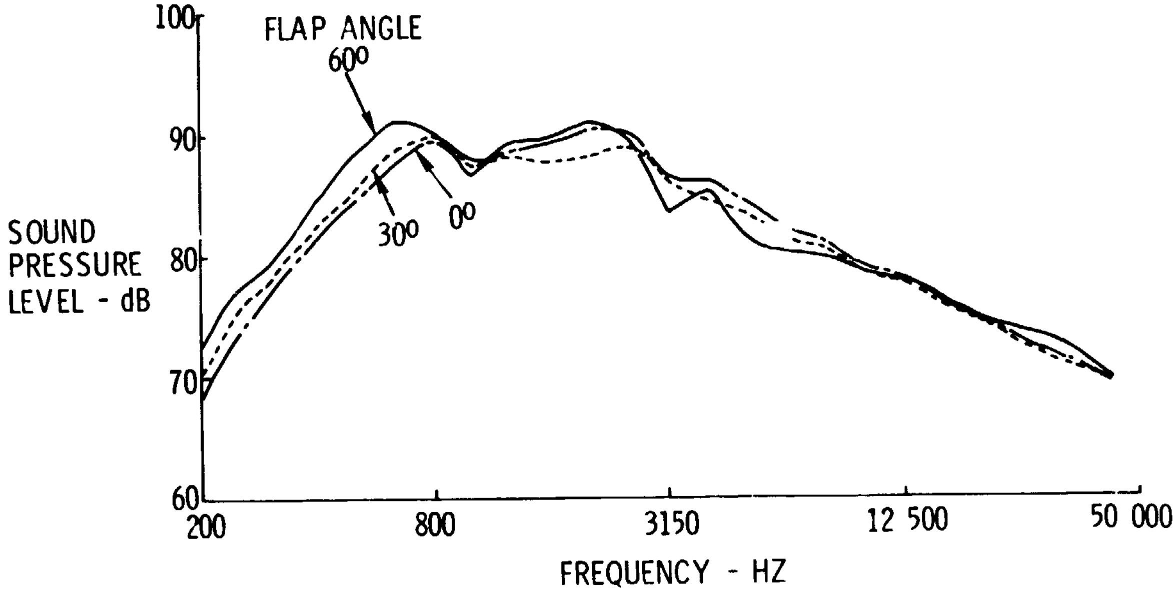

Figure 8.- Effect of flap angle. Jet velocity 215 m/s; AR4 nozzle; nozzle location 20% chord; nozzle impingement angle 20°.

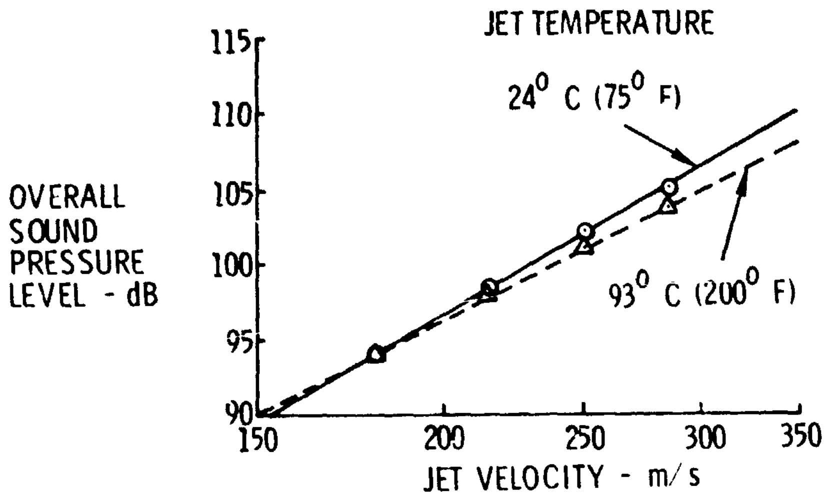

Figure 9.- Temperature trends. AR4 nozzle; nozzle impingement angle 20°; nozzle location 20% chord; flap angle 30°.

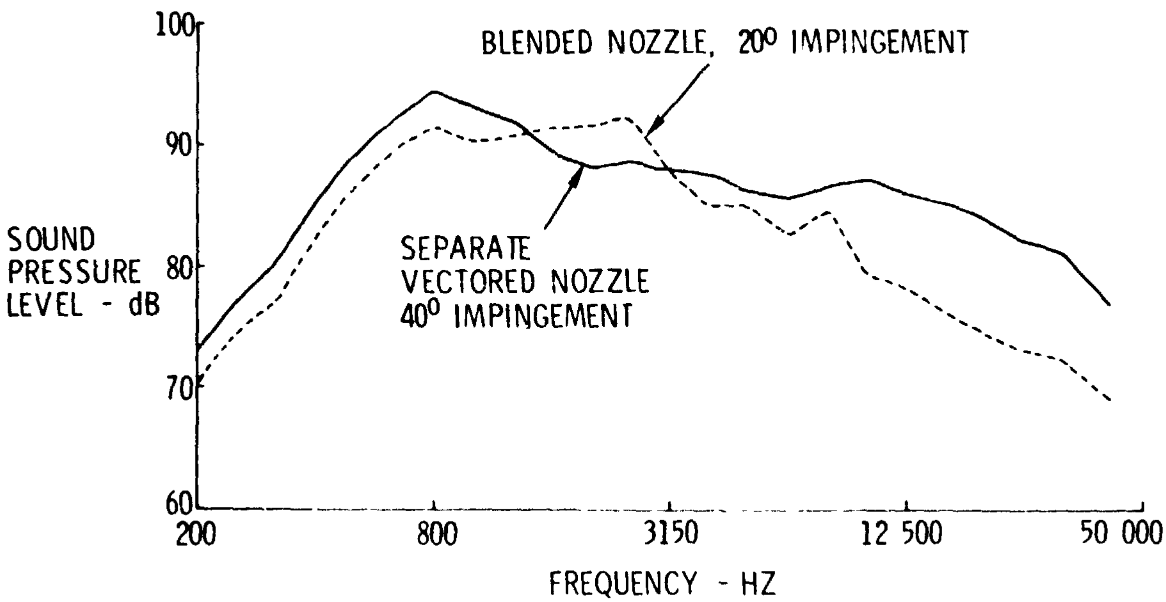

Figure 10.- Vectored thrust trends. Jet velocity 215 m/s; round nozzle; nozzle location 20% chord; flap angle 30°.

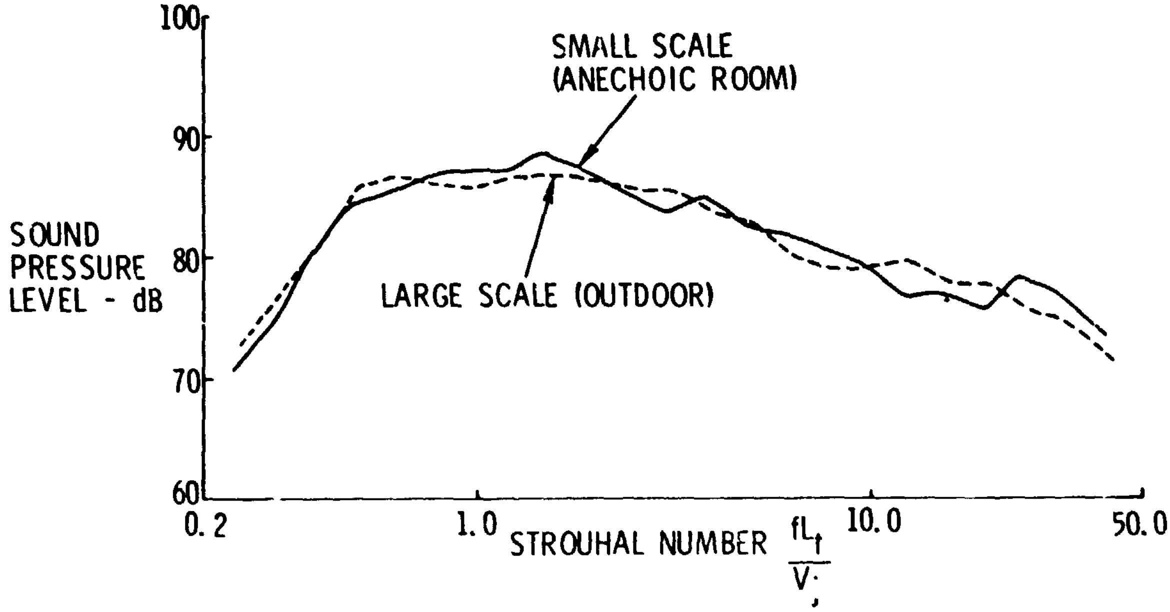

Figure 11.- Scaling results. Jet velocity 215 m/s; AR8 nozzle; nozzle impingement angle 20°; nozzle location 20% chord; flap angle 30°.

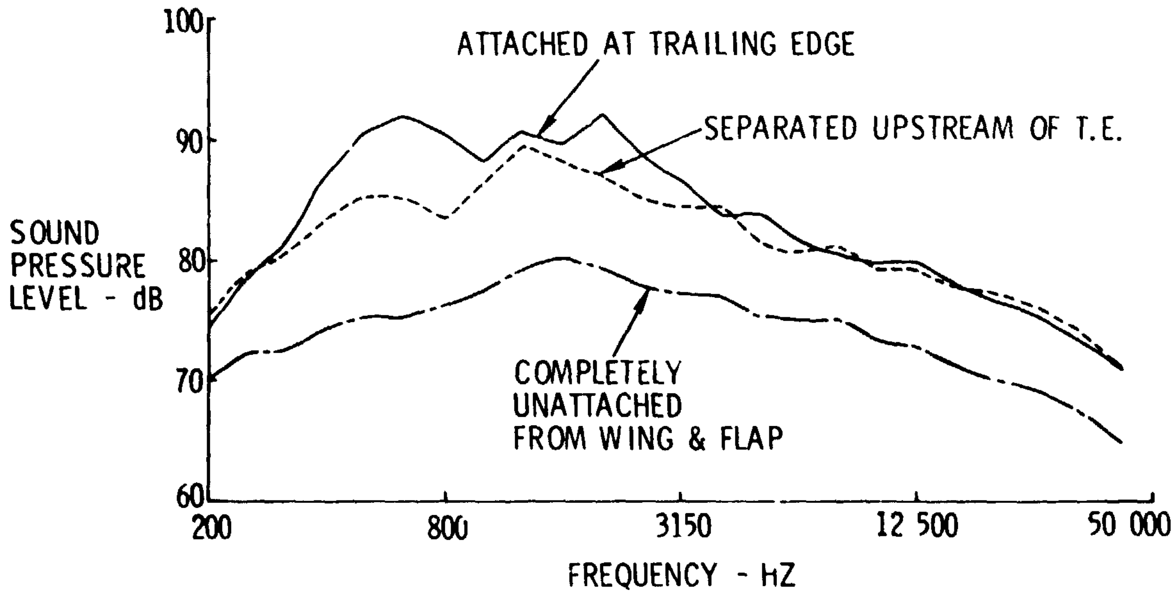

Figure 12.- Effect of flow attachment. Jet velocity 215 m/s; AR8 nozzle; nozzle location 20% chord.

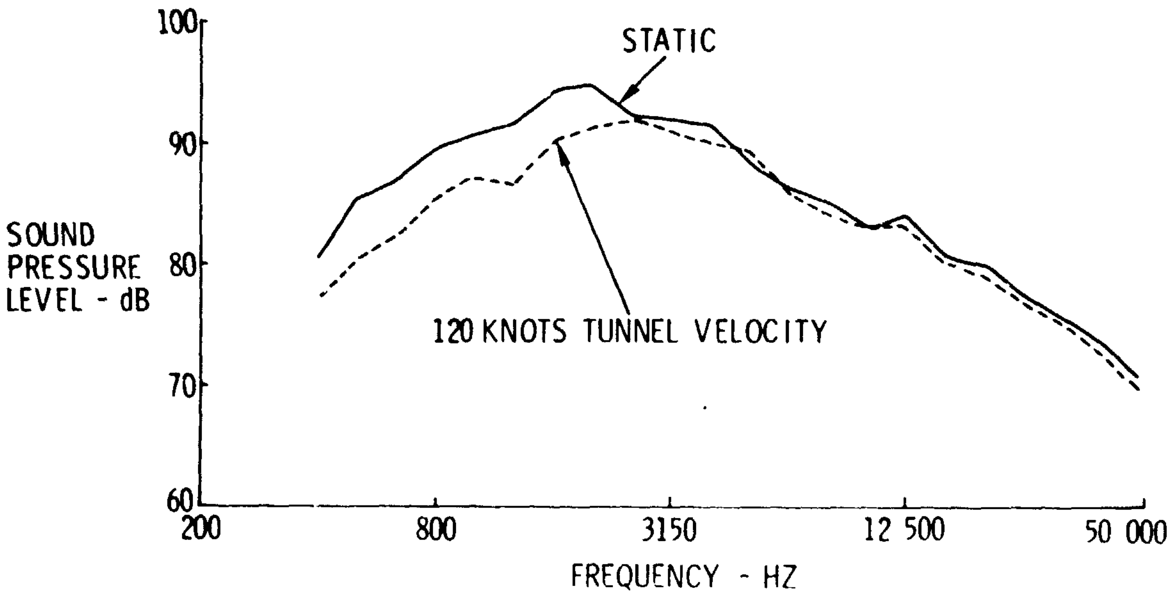

Figure 13.- Wind tunnel trends. Jet velocity 250 m/s; AR2 nozzle; nozzle location 20% chord; nozzle impingement angle 20°; flap angle 30°.